

Real-time implementation of a measurement-based adaptive wide-area control system considering communication delays

S. Ray and G.K. Venayagamoorthy

Abstract: A wide-area control system (WACS) uses wide-area measurement signals to provide auxiliary stabilising controls to power system devices. An adaptive WACS has been designed to provide damping control signals to the excitations of generators. The delays in signal transmission and the reliability of the communication network is a major concern with wide-area measurement-based control. The adaptive WACS is designed to compensate for a wide range of communication delays and provide robust damping to mitigate system oscillations. A single simultaneous recurrent neural network is used in the realisation of the adaptive WACS for both identification and control of the power system. The WACS has been implemented on a digital signal processor and its performance is evaluated on a power system implemented on a real-time platform – the real-time digital simulator. The additional damping provided by the WACS is enumerated using Prony analysis.

1 Introduction

Large interconnected power systems are the basis of modern life. The number of bulk power exchanges over long distances has increased as a consequence of deregulation of the electric power industry. Several measures have been taken in recent decades to provide better stability and reliability to stressed systems. Slow-mode oscillations are among the major concerns for stability of the entire power system. Thus, local compensators such as power system stabiliser (PSS) and flexible alternating current transmission systems (FACTS) are installed on different sections of power systems to provide damping.

Local controllers have good performance when local measurements provide all information about the dynamics of disturbances. But, if there are adverse interactions between multiple adjacent areas of the power system, a wide-area-based measurement provides better stabilising control [1–5]. A wide-area control system (WACS) coordinates the actions of distributed agents using supervisory control and data acquisition (SCADA), phasor measurement unit or other sources that provide wide-area dynamic information [6–9]. The WACS receives information/data from different areas in the power system and, based on some pre-defined objective function, sends appropriate control signals to distributed agents for enhancing system's dynamic performance [1–9]. The design and implementation aspects of a SCADA-based wide-area monitoring and control system is explained in [7, 9–10].

Multiple-linear model-based adaptive and hierarchical wide-area control for damping post-disturbance oscillations have been reported [11, 12]. The wide-area measurement-

based control suffers from signal transmission delays [13]. Linear matrix inequality (LMI), gain scheduling and H^∞ -based WACS have been used to provide effective auxiliary damping control accounting signal transmission delays [14–17]. Feedback delays ranging from 50 ms to 1.0 s have been compensated using different classical techniques for PSSs [14–16], FACTS devices such as static var compensators and thyristor controlled series compensators [17]. In [18], the implementation of a similar WACS is reported on a real-time platform (RedHawk RT-Linux operating system on a dual-Xeon processor) with a time step of 1–10 ms and without considering any signal transmission delays. All these designs require a mathematical model of the system, which is difficult to implement in practice. An alternative solution is a measurement-based design.

In a recent study, an intelligent and adaptive modern power grid has been envisioned with intelligence built-in controllers, that will provide fast and accurate action during contingencies [19]. Neural networks, known also as intelligent agents, are universal approximators that are able to identify and control multiple-input–multiple-output (MIMO) time-varying systems like turbogenerators based on input–output measurements [20, 21].

This paper presents the design and real-time implementation of an intelligent adaptive wide-area controller based on measurements. The primary contributions of this paper are:

- design of an adaptive WACS to provide auxiliary damping to generators through their excitations;
- compensation of transmission delays ranging from 0 to 1.4 s in measured and control signals;
- the use of a single simultaneous recurrent neural network (SRN) for both identification and control functions for the WACS design and
- demonstration of the real-time implementation of the proposed WACS on a digital signal processor (DSP) interfaced to the real-time digital simulator (RTDS).

2 Multi-machine power system with WACS

A power system is a complex network with thousands of buses, several hundreds of generators and interactions between multiple areas with several inter-area modes of oscillations. The two-area power system [22, 23] of Fig. 1 is a test system, commonly used to show the effectiveness of controllers in damping slow-mode oscillations. It is important to demonstrate that the real-time implementation of the adaptive WACS is practical; therefore this system is chosen because of the limitation of the existing real-time implementation platform (RTDS) in the Real-Time Power and Intelligent Systems laboratory, but the concept is applicable to any power system. The RTDS simulator platform is explained in Section 4 [24].

A two-area system with the WACS shown in Fig. 1 consists of two fully symmetrical areas linked together by two transmission lines. Each area is equipped with two identical synchronous generators rated 20 kV/900 MVA. All the generators are equipped with identical speed governors and turbines, AVRs and excitors (Fig. 2). The switch S1 (Fig. 2) can be used to provide auxiliary control signals to the generators. The switch S2 (Fig. 2) is used to add the PSS signal to the excitation system. Generators G1 and G3 are only equipped with PSSs. Loads are represented as constant impedances and split between the two areas in such a way that Area 1 transfers ~413 MW to Area 2. Three electromechanical modes of oscillation are present in this system: two inter-plant/intra-area modes, one in each area, and one inter-area low-frequency mode [23]. The parameters of the two-area system are given in [23].

3 Adaptive WACS

The WACS actions are based on remote signal measurements from different areas. These remote signals are exchanged over communication channels that have transmission delays. This results in late arrival of the measured signals by τ_1 s at the wide-area control station. Thus, the actions taken by the WACS based on these signals are no longer valid for the current state of the system. Similarly, the control signals of the WACS communicated to the respective areas/generators also arrive late by τ_2 s. Hence, the stabilising control signal generated by the WACS is out of phase and it adversely affects the stability of the system. As mentioned in Section 1, the WACS design is

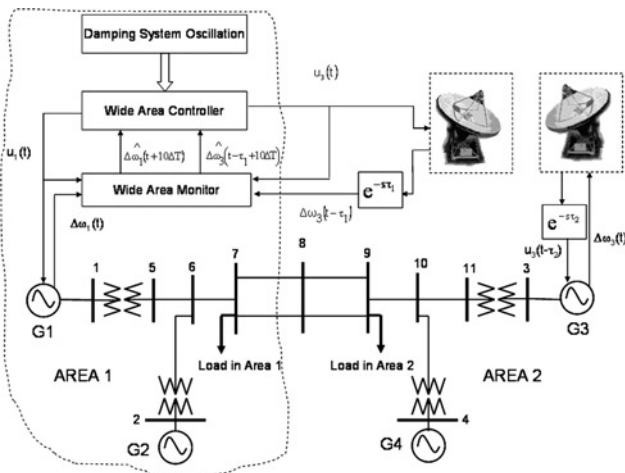


Fig. 1 Two-area power system with a WACS considering signal transmission delays

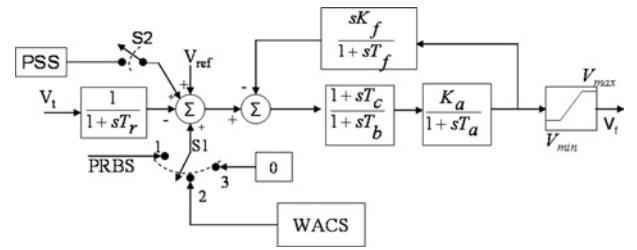


Fig. 2 Block diagram of the AVR-exciter model

needed to provide stabilising control despite a substantial delay in the communication of both measurement and control signals. In this study, it is assumed that the WACS can be located in one of the areas to eliminate delays in at least one set of measurement and control signals. For the two-area system in Fig. 1, the WACS is located in Area 1. Thus, the delays are in communicating generator G3's speed deviation signal to the WACS, and the WACS communicating the damping control signal to generator G3 in Area 2. The objective of the WACS is to provide satisfactory damping signals for a wide range of communication delays. According to previous papers [14–17], the delay in communication channels and in sensor measurements are typically in the range of 50 ms to 1.0 s. For additional delays, the signal is considered to be missing. Hence, taking the maximum delay, the WACS has been designed for a maximum delay of 1.0 s though, during testing, satisfactory performance was achieved up to a delay of 1.4 s. The WACS design is based on a single SRN [25]. The SRN is used to provide an accurate representation of the system dynamics at all time instances and subsequently to generate appropriate control signals to damp oscillations.

3.1 Simultaneous recurrent neural network

SRNs are robust and ideal for multi-step predictions. The SRN is a dynamic or recurrent structure in which the outputs depend on the inputs to the SRN and partially or fully on the outputs of the different layers of the SRN. The difference between a conventional recurrent neural network (RNN) and SRN is that the feedbacks are time delayed in RNNs whereas instantaneous in SRNs. In the implementation of the SRN, much higher sampling rates are used to emulate instantaneous feedback. To implement an SRN in real-time, the simultaneous recurrences have to be done multiple times within one sampling period of the system measurements. Hence, for ten simultaneous recurrences, the outputs of the SRN hidden layer need to be calculated 10 times and fed back as inputs to the hidden neurons. Hence, to achieve this methodology, the SRN calculated is 10 times per sampling period of 0.1 s; thereby, the internal sampling rate used for the SRN is 100 Hz. The output of a typical SRN is given by (1)

$$\bar{y} = W_2 \cdot \bar{d} \quad (1)$$

where

$$\bar{d} = \frac{1}{1 + e^{-\bar{a}}} \quad (2)$$

and $\bar{a} = W_1 \bar{X}$ is the input vector to the hidden layer, $\bar{X} = [x, 1, \bar{d}]^T$ the input vector, \bar{d} the output of the hidden layer, \bar{y} the output vector, W_1 the input weight matrix and W_2 is the

output weight matrix. More details on the SRNs can be found in [25, 26].

3.2 Training of WACS

The design of the adaptive WACS is based on an adaptive control method [27, 28]. Owing to the nonlinearity and time-varying nature of the power system, this control method requires a model/identifier to represent the power system dynamics accurately from moment to moment thus requiring online training. In this paper, a single SRN is used for both identification and control in the adaptive WACS design. The SRN operates in the forward mode as an identifier and in the reverse mode as a controller. It should be noted that the WACS parameters may not always be updated, provided it is trained for steady state as well as transients for different operating conditions of the system.

To minimise the adverse effects of signal transmission delays from the wide-area measurements, the WACS (in the forward mode) is trained to predict the speed deviation of the generators several steps ahead, ten steps in this paper. As in the classical methods for power system identification [29], the WACS is initially trained with small amplitude pseudo-random binary signals (PRBS) (up to $\pm 10\%$) that are added to the excitation inputs of generators G1 and G3 (with switch S1 in Fig. 2 in position 1). The PRBS signal excites all possible dynamics of the power system. During this initial training period, the SRN is trained with higher learning rate (0.06) for 40 min at the sampling rate of 10 Hz. After the weights of the SRN stabilise, the SRN training is continued with a small learning rate of 0.001 while in closed loop operations. During the online operation, the WACS outputs are applied to the excitation systems of G1 and G3 (switch S1 in Fig. 2 in position 2) and the online training of the SRN can be continued with a small learning rate. Online training means that the SRN is trained at each sampling instance using the signals measured from the system on-the-fly. In practical applications, PRBS signals can be substituted with different low signal-to-noise ratio probing signals [29]. The ambient measurements exhibit small oscillations in the system because of small changes in generation, loads and operating conditions, which can also be utilised to identify the modes of the system [30]. In most of the neural network-based identification, a probing signal-based excitation is preferred to other methods if possible [20]. To investigate the ambient measurement-based training technique, random load changes of $\pm 10\%$ of total installed load is also carried out to train the controller, and corresponding results are given in case study 5. The input layer of the SRN consists of 41 inputs [measured speed deviations $\Delta\omega_1$ and $\Delta\omega_3$, and exciter input (see Appendix) voltages u_1 and u_3 of generators G1 and G3, respectively, received by WACS at time t , $(t - \Delta T)$, \dots , $(t - T)$ and a bias term] in which ΔT is the sampling period. The hidden and output layers consist of ten sigmoidal and two linear neurons, respectively. The outputs of the WACS in the forward mode are estimated speed deviations $\Delta\hat{\omega}_1(t + 10\Delta T)$ and $\Delta\hat{\omega}_3(t + 10\Delta T)$ of the generators G1 and G3, respectively, ten sampling periods ahead. Pruning techniques are used to obtain the minimum number of hidden neurons for the SRN. The complete SRN is composed of input weight W_1 [10×51], output weight W_2 [2×10], input vector X [51×1], hidden layer output vector d [10×1] and output vector y [2×1].

In practical systems, there may be several individual generators connected to one bus or distributed in one area, but

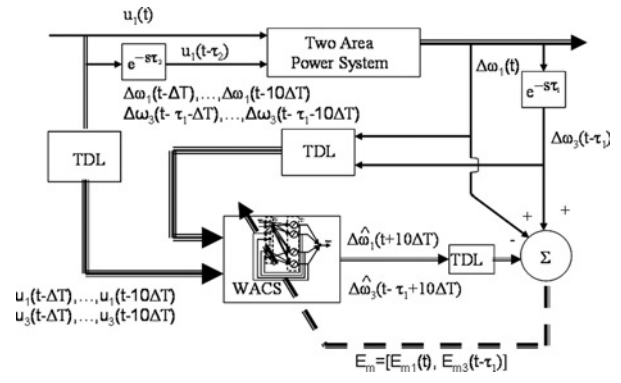


Fig. 3 WACS training schematic (TDL, time-delayed lines)

as the generators within one area are coherent, the measurements from the dominant generator can be used for inputs to the WACS. The WACS output can be fed either to the excitation system of the dominant generator contributing to the inter-area mode or to all the generators' excitations within one area depending on the feasibility and cost of implementation. The modal observability of measured states is critical for damping inter-area oscillations. The schematic for the WACS inputs, outputs and training is illustrated in Fig. 3. The objective of the training is to minimise the square of the error $E_m(t)$ in (3) by using (4) and (5) where α ($0 < \alpha < 1$) is the learning rate. The learning rate during initial training used in this paper is 0.06 whereas during continuous online training under operation, it is reduced to 0.001.

$$E_m(t) = \Delta\omega(t) - \Delta\hat{\omega}(t) \quad (3)$$

$$w_1(t + 1) = W_1(t) + \alpha \frac{\partial E_m(t)}{\partial W_1(t)} \quad (4)$$

$$W_2(t + 1) = W_2(t) + \alpha \frac{\partial E_m(t)}{\partial W_2(t)} \quad (5)$$

3.3 Operation of WACS

The control signals (WACS operating in the reverse mode) are generated using the difference between the outputs of a desired response predictor (DRP) and the outputs of the WACS in the forward mode, as shown in Fig. 4. The two control signals, u_1 and u_3 , are the auxiliary signals (7) added to generators G1 and G3's excitation systems, respectively, using the switch S1 in position 2 (Fig. 2). The low-pass filter is used to eliminate high-frequency

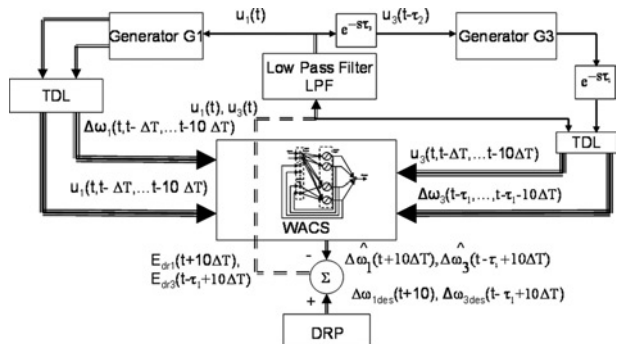


Fig. 4 Operation mode of the WACS

components and smooth out the control signals generated with a sampling frequency (10 Hz). The desired responses for the speed deviations ten sampling periods ahead, $\Delta\omega_{1\text{des}}(t + 10\Delta T)$ and $\Delta\omega_{3\text{des}}(t - \tau_1 + 10\Delta T)$, are taken to be a weighted summation of the past speed deviations. This desired trajectory provides a step-by-step transition in getting the speed deviations to zero as reported in [21, 27, 28]. The DRP represents a desired linear model, which satisfies required specifications of damping performance. The control actions are generated such that it cancels the nonlinearity of the original system and tracks the response of the desired linear model, thus providing damping. The DRP is given in (6)

$$\Delta\omega_{1\text{des}}(t + 10\Delta T) = - \sum_{i=0}^{i=N} A_i \Delta\hat{\omega}_1(t - i\Delta T) \quad (6)$$

$$\Delta\omega_{3\text{des}}(t - \tau_1 + 10\Delta T) = - \sum_{i=0}^{i=N} A_i \Delta\hat{\omega}_3(t - \tau_1 - i\Delta T)$$

$\Delta\hat{\omega}_1(t)$ and $\Delta\hat{\omega}_3(t)$ are the outputs of the neuro-identifier or model at time t . In this DRP design, the parameters are chosen as $N = 3$, $A_0 = 3.04$, $A_1 = -3.883$, $A_2 = 2.422$ and $A_3 = -0.6416$. The dominant poles of the desired linear model in the discrete domain are located at $(0.8511 + 0.3557i)$, $(0.8511 - 0.3557i)$, $(0.6691 + 0.5536i)$ and $(0.669167 - 0.5536i)$. As the poles are within the unit circle, the system is asymptotically stable. The discrete desired pole locations are found by converting the desired continuous pole locations to discrete using 0.1 s as the sampling frequency. The desired continuous linear model is chosen to provide a damping of 0.2 for both inter-area 0.63 Hz and intra-area 1.1 Hz modes. The error between the desired and the actual speed deviations are backpropagated through the WACS network and the differentiation of the errors with respect to the control inputs (V_r) of the WACS yields desired control signals, $u_1(t)$ and $u_3(t)$ as expressed in (7)

$$u_1(t) = \frac{\partial E_{\text{dr1}}(t + 10)}{\partial V_r(t)} \quad (7)$$

$$u_3(t) = \frac{\partial E_{\text{dr3}}(t - \tau_1 + 10)}{\partial V_r(t)}$$

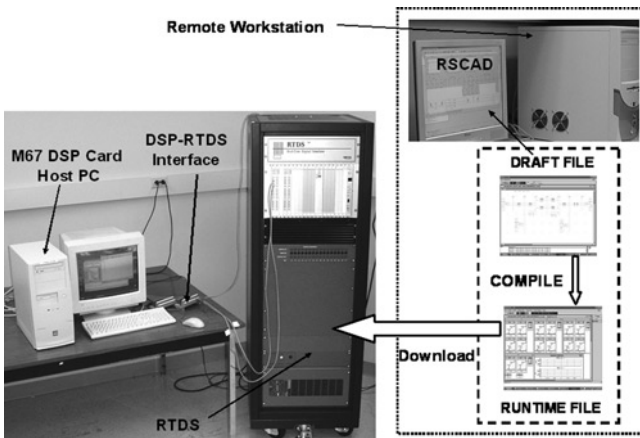


Fig. 5 Laboratory hardware setup, DSP and the RTDS

3.4 Implementation of wide area controller

The implementation of the controller is done in the reverse mode using the error backpropagation method used to train neural networks. The error between the DRP output and the WACS output, given by (8), is backpropagated from the output layer to the hidden layer, and then from the hidden layer to the input layer of the SRN, as given in (9) and (10) to generate the control signals given in (11).

$$\text{err}_1 = \Delta\omega_{1\text{des}}(t + 10\Delta T) - \Delta\hat{\omega}_1(t + 10\Delta T) \quad (8)$$

$$\text{err}_2 = \Delta\omega_{3\text{des}}(t + 10\Delta T) - \Delta\hat{\omega}_3(t + 10\Delta T)$$

$$\text{ed}_i = \frac{\partial \overline{\text{err}}}{\partial d_i} = \sum_{j=1}^2 W_{2ji} \text{err}_j, \quad i = 1, \dots, N \quad (9)$$

$$\text{ea}_i = \frac{\partial \overline{\text{err}}}{\partial a_i} = d_i(1 - d_i)\text{ed}_i, \quad i = 1, \dots, N \quad (10)$$

$$u_1 = \sum_{j=1}^N W_{13j} \text{ea}_j \quad (11)$$

$$u_3 = \sum_{j=1}^N W_{14j} \text{ea}_j$$

where N is the number of neurons in the hidden layer, ed the derivatives of error in the output layer with respect to output of the hidden layer and ea the derivative of error in the output layer with respect to the input of the hidden layer. The generated control signal is applied to the excitation of generators G1 and G3, and the SRN is continuously trained with past inputs and outputs with a small learning rate (typically 0.001).

4 Real-time implementation platform

Owing to its complexity and expensive nature, it is very difficult to test new control methods and algorithms on a real-world power system. The proposed WACS is implemented on a DSP and its performance is tested on the two-area power system simulated on a real-time power system simulation platform, the RTDS. The RTDS is a fully digital power system simulator capable of continuous real-time operation. It performs electromagnetic transient power

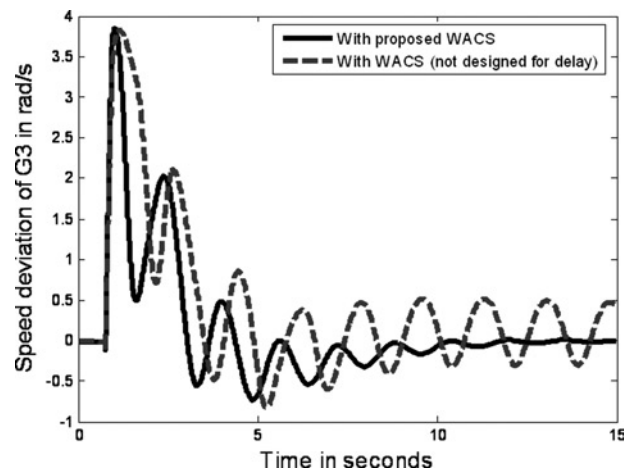


Fig. 6 Speed deviation of generator G3 with the proposed controller and WACS not designed for the delays for a three-phase short circuit at bus 10 (Fig. 1) for ten cycles (166.67 ms) duration

system simulations with a typical time step of 50 μs utilising a combination of custom software and hardware. The proprietary operating system used by the RTDS guarantees 'hard real time' during all simulations [24]. It is an ideal tool for the design, development and testing of power system protection and control devices.

With a large capacity for both digital and analogue signal exchange (through numerous dedicated, high-speed I/O ports), physical protection and control devices can be connected to the simulator to interact with the simulated power system. The WACS is implemented on the Innovative Integration M67 DSP card (based on the TMS3206701 processor), operating at 160 MHz, hosted on a Pentium III 433 MHz personal computer. The M67 DSP card is equipped with two A4D4 modules [31]. Each A4D4 module is equipped with four analogue-to-digital converters and four digital-to-analogue converters. The DSP (implements WACS) and RTDS (implements power system) interface and laboratory hardware setup is shown in Fig. 5.

5 Evaluation of WACS damping performance

Performance of the WACS is evaluated and compared with performance of the PSSs for small and large disturbances

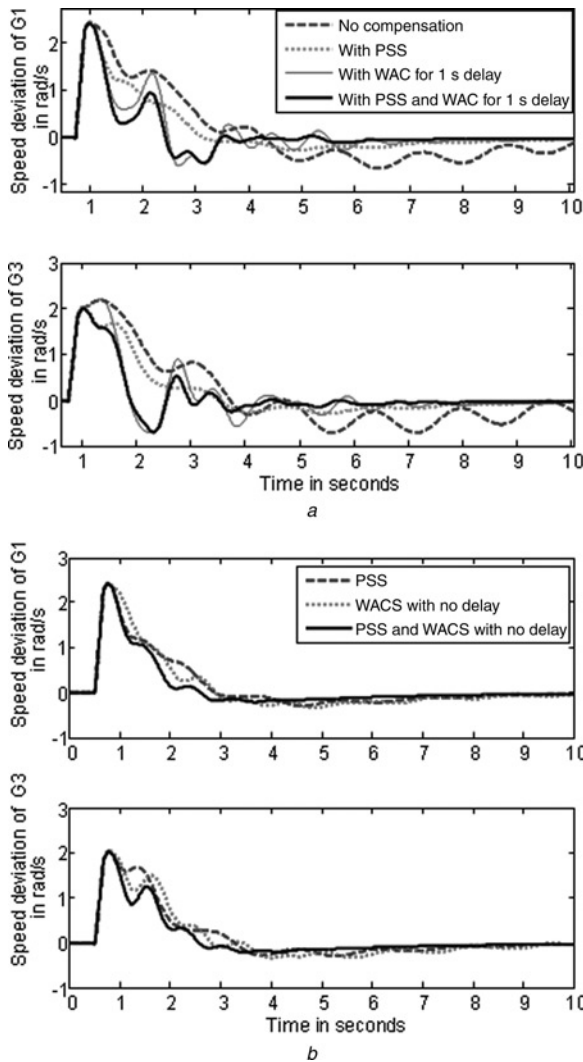


Fig. 7 Speed deviation of generators $G1$ and $G3$

a For different controller combination for a three-phase short circuit at bus 8 (Fig. 1) for ten cycles (166.67 ms) duration
b With different controllers for a ten-cycle (166.67 ms) three-phase short circuit at bus 8 with no delay in signal transmission

applied to the power system. The case studies carried out are given in Section 5.1. Prony analysis on the performance of the WACS is given in Section 5.2. This section also quantifies the transient energy exhibited by the generators ($G1$ and $G3$) under different disturbances with only PSSs and the combination of PSS and WACS.

5.1 Case studies

The WACS provides auxiliary damping signals to the excitations systems of generators $G1$ and $G3$ when there is a power swing in either one or both areas. The outputs of the WACS are zero under steady-state condition. Five case studies are carried out as explained below.

Case Study 1: Fig. 6 shows the typical responses of the system for a ten-cycle three-phase line to ground short-circuit fault applied at bus 10 considering signal transmission delays with a WACS not designed to compensate for time delays and a WACS designed to compensate for time delays, respectively. With the WACS not designed to compensate for delays, there are sustained oscillations. The WACS signal causes adverse effects on the overall system unlike the WACS design considering delays which damps out the electromechanical slow mode of oscillations.

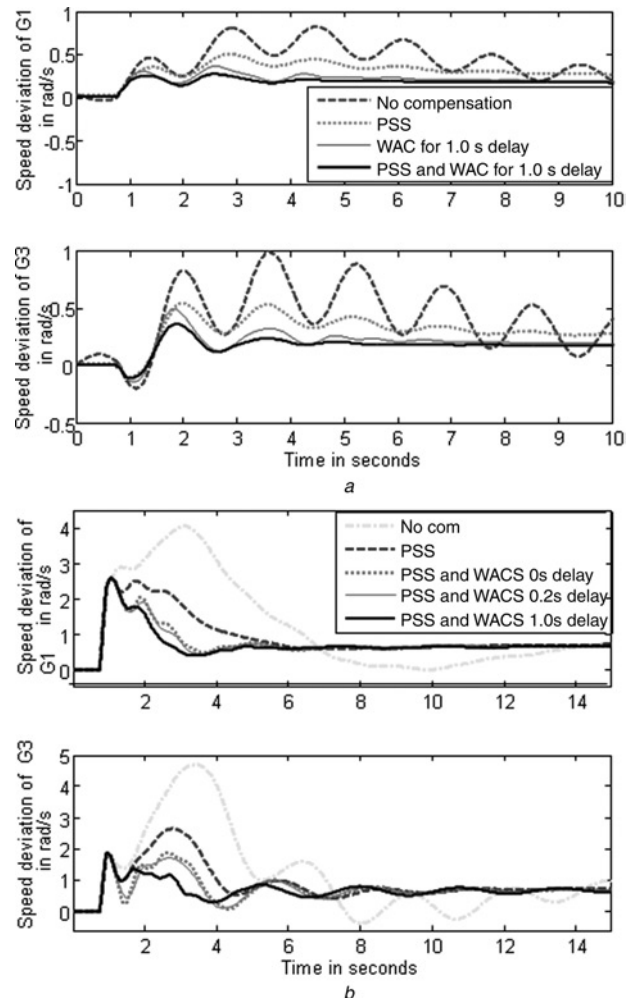


Fig. 8 Speed deviation of generators $G1$ and $G3$

a For different controller combination for a load decrease in Area 1 and an increase in Area 2 (Fig. 1)
b For different controllers and various delays in signal transmission for a ten cycles (166.67 ms) three-phase short circuit at bus 8, which is cleared by opening one of the parallel lines between buses 7 and 8 and buses 8 and 9

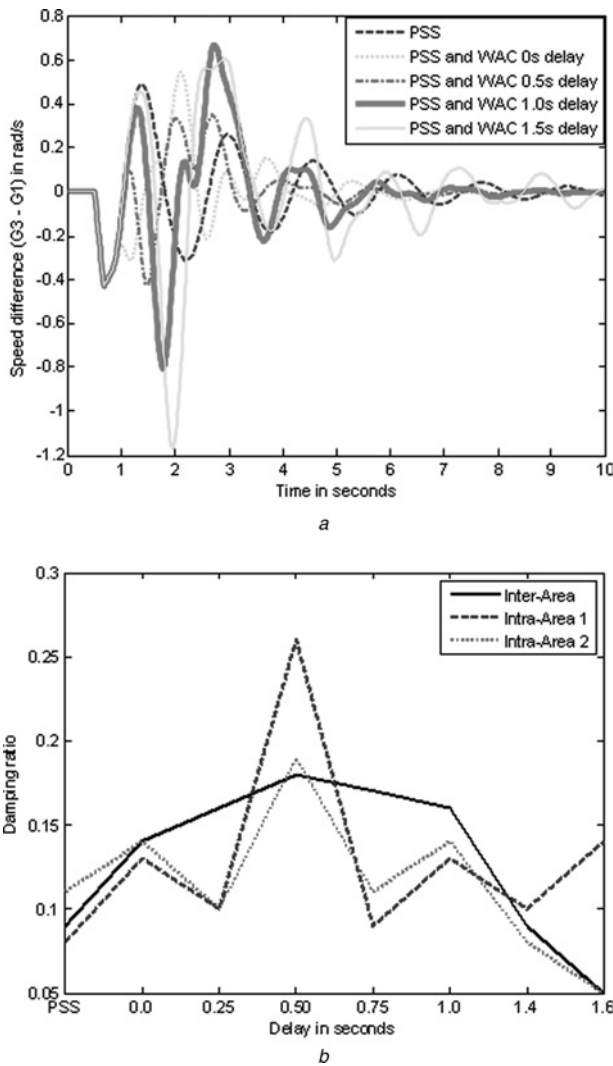


Fig. 9 Speed deviation of generators and performance with PSS and WACS for different delays

a Speed deviation of generators G3 with respect to G1 ($\omega_3 - \omega_1$) with different signal transmission delays for a three-phase ten cycles (166.67 ms) duration short circuit at bus 8 (Fig. 1)

b Damping of different modes for PSS and PSS and WACS with various communication delays

Case Study 2: A three-phase short circuit is applied at bus 8 for the duration of ten cycles (166.67 ms). Fig. 7 shows the speed deviations of generators G1 and G3 with no PSS (Uncompensated, dotted-line), with PSS on G1 and G3 (dashed-line), with only the WACS (solid line) and, with the PSS and the WACS on generators G1 and G3 (solid bold line) without any delay in signal transmission (Fig. 7a) and with a delay of 1.0 s in wide-area measurement and control (Fig. 7b). It is clear from this figure that though the WACS itself does not show much better response than PSSs, the combination of PSS and the WACS (solid bold line) exhibit superior performance.

Prony analysis in Section 5.2 shows that though the WACS itself can mitigate inter-area modes, there exists some intra-area or local modes which are not damped as well as the inter-area modes without the PSS. This is because the WACS training is done with the PSSs online. Hence, without any PSS, the WACS may not be able to provide appropriate damping to the intra-area or local modes for the controller design presented in this paper. The WACS performs as a supplementary controller in this study. But, from the results and Prony analysis, it can be concluded that the WACS signal provide better performance even without PSSs.

Case Study 3: Fig. 8a shows the speed deviation of generators G1 and G3 for load changes in Areas 1 and 2. The load in Area 1 is decreased from 967 – j100 to 870 – j90 MVA and the load in Area 2 is increased from 1767 – j250 to 1863 – j260 MVA. It can be observed that PSSs, the WACS and combined PSS and the WACS, all stabilise the power system. The WACS and PSSs combination damp out oscillations faster. There is a small steady-state error in the speed response causing a 0.05 and 0.07% change in the frequency of generators G1 and G3, respectively, due to a load change in the areas. This is as a result of the speed governors having a 5% droop setting. Fig. 8b presents a contingency where the post-fault topology of the system changes. A three-phase line-to-ground short circuit is applied at bus 8 for ten cycles and cleared by opening one of the parallel lines between buses 7 and 8 and buses 8 and 9. Except for the extreme condition of 1.0 s communication delay, the combination of PSS and WACS provides a good response for the change in topology. Thus, the controller shows robustness to situations with no prior knowledge.

Case Study 4: To verify the robustness of the proposed design, a ten-cycle three-phase line-to-ground short circuit is applied at bus 8. The transmission delays for the WACS measurement (τ_1) and control signals (τ_2) are varied from zero to a maximum of 1.5 s. Fig. 9a exhibits acceptable controller performance of PSS and WACS for a wide range of transmission delays. A graphical comparison of damping of one inter-area and two intra-area modes with respect to different transmission delays in WACS communication is also presented in Fig. 9b.

Along with these figures, the transient energies of the generators (G1 and G3) in the first 15 s after the faults are computed using (12)

$$TE_{GEN_i} = \frac{1}{2} H_{GEN_i} \int_{t_{fit}}^{t_{fit}+15} \Delta\omega_i^2 dt \quad (12)$$

where i is the generator number and t_{fit} the time the fault is triggered. Table 1 presents the transient energies of generators G1 and G3 because of a short-circuit fault at bus 10 for 167 ms. Calculations show observable improvement in the transient energies of each generator with the WACS signals under variable signal-transmission delays. The transient energies of generators G1 and G3 because of a

Table 1: Transient energy of generators 1 and 3 for different stability agents

Generators	Transient Energy in MJ No compensation	PSS	PSS and WACS 0.5 s delay	1.0 s delay	1.4 s delay
G 1	51.47	26.86	19.77	19.44	22.00
G 3	64.85	30.33	26.20	22.51	24.89

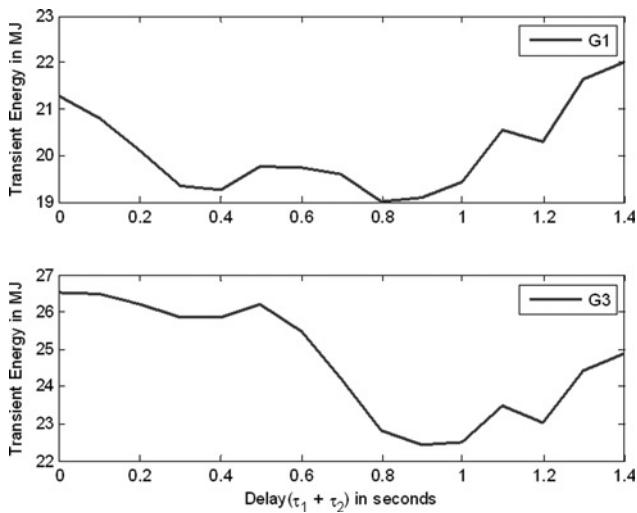


Fig. 10 Transient energy of generators G1 and G3 for different delays in the wide-area measurement and control signals

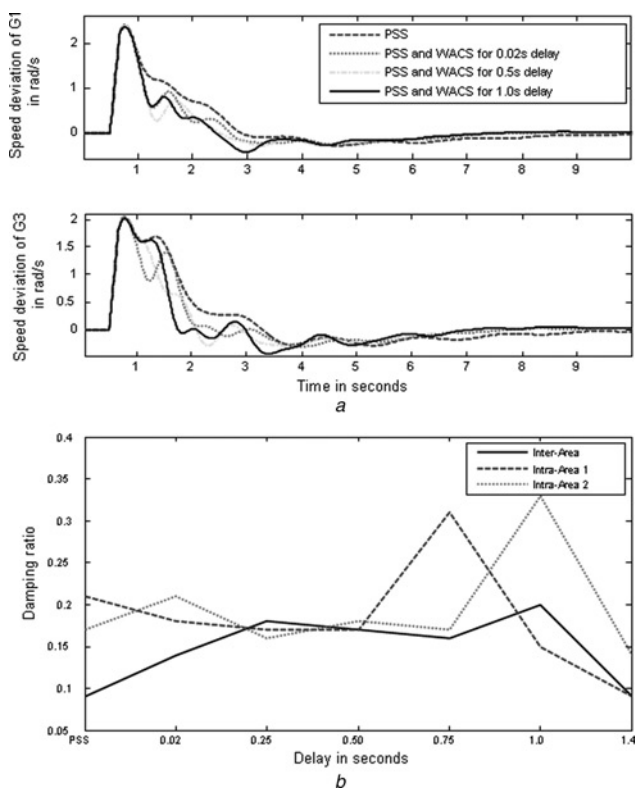


Fig. 11 Speed of generators and damping ratios for different delays

a Speed of generators G1 and G3 for 10-cycle short-circuit fault at bus 8- the WACS trained with ambient measurements
 b Damping ratios of inter-area and intra-area modes for the WACS trained with ambient measurements

short-circuit fault (ten cycles) for different signal transmission delays ($\tau_1 + \tau_2$), ranging from 0 to 1.4 s, are shown in Fig. 10. The performance of the WACS design is seen to be robust for variable delays.

Case Study 5: To investigate the possibility of training the controller with ambient measurements, random load changes within $\pm 10\%$ of normal loading is simulated and the SRN is trained in a similar fashion as given in Section 3. The same number of input, output and hidden neurons are used with a learning rate of 0.05 for ~ 3 h. The controller performance is tested using different delays in communication signal for a three-phase line-to-ground short-circuit fault for ten cycles (166.67 ms). The speed of generators G1 and G3 is presented in Fig. 11a. The damping ratios for different delays with PSS and WACS combined are also presented in Fig. 11b. Although the SRN initially takes more time to train with ambient measurements, results show that the trained SRN WACS performs equally well, compared with the controller trained with PRBS. For a practical real-world system, ambient measurements may provide a better option for training the WACS.

5.2 Stability analysis with the Prony method

Prony analysis [32, 33] is an extension of Fourier analysis and it helps to find the modal contents by estimating frequency, damping and phase of a signal. This analysis tool is useful to provide information on the stability of the system at the operating point of concern without any need of extensive techniques to linearise the complete system model. The analysis is performed on the measured data; hence, no prior information regarding the system is required. The real-time implementation platform consisting of RTDS and DSP does not provide any means to obtain the linearised closed-loop model of the system. Therefore to illustrate and quantify the improvement with the WACS design in terms of damping ratios, the Prony method is chosen. Although for different delays the linear models obtained from the Prony analysis are different, Table 2 presents the results for a signal transmission delay of 1.0 s. This method is applied on the speed data of generators G1. The frequency and damping of each dominant mode is given in Table 2. It can be seen that the designed adaptive WACS improves the stability of the system even with the signal transmission delays in both measurement and control signals. The design is based on the measurement data and no prior information is used in this design. For a system with multiple modes of oscillations, during initial training phase, the WACS identifies slow modes of the system. Thus, the WACS design with the SRN demonstrated on a two-area power system is equally applicable to larger systems with several modes of oscillations. The SRN network will identify the complex modes and

Table 2: Frequency and damping of the system for different power system stability controllers

No compensation		With PSS		With WACS		With PSS and WACS	
f , Hz	ζ	f , Hz	ζ	f , Hz	ζ	f , Hz	ζ
0.61	0.01	0.62	0.09	0.63	0.22	0.57	0.23
1.22	0.07	1.23	0.1	1.19	0.08	1.20	0.18
1.17	0.07	1.30	0.09	1.20	0.09	1.15	0.09

provide damping to the power system when operating in reverse mode.

6 Conclusions

This paper has presented the design of an adaptive WACS for damping generator oscillations by providing auxiliary signals to their excitation systems. This WACS is designed to compensate for transmission delays ranging from 0 to 1.4 s with satisfactory performance. The WACS is realised with a single SRN, which serves a dual purpose of continuous identification of the power system dynamics and generation of appropriate damping control signals. This type of design has merit in that it can provide damping for several modes of oscillations. Real-time implementation on the RTDS and DSP platform demonstrates the feasibility of practical realisation of a wide-area measurement-based SRN control system for a two-area four machine power network. Multiple SRNs or ObjectNets implemented on a number of high-speed processors will be needed to realise this type of control system for large power networks.

The results with the WACS show better damping of system oscillations caused by small and large disturbances over a wide range of operating conditions. The combination of PSS with WACS provides superior damping to the inter-area as well as intra-area oscillating modes for the test system in this paper. This superior WACS performance is substantiated with eigenvalue analysis of the closed-loop system. This adaptive WACS design shown on a small power system is a promising and potential measurement-based technique for large power systems.

7 Acknowledgment

The financial support from the National Science Foundation, USA under the grant CAREER ECCS # 0348221 is gratefully acknowledged by the authors.

8 References

- 1 Ni, H., and Heydt, G.T.: 'Power system stability agents using robust wide area control', *IEEE Trans. Power Syst.*, 2002, **17**, (4), pp. 1123–1131
- 2 Taylor, C.W., Erickson, D.C., Martin, K.E., Wilson, R.E., and Venkatasubramanian, V.: 'WACS-wide area stability and voltage control system: R & D and online demonstration', *Proc. IEEE*, 2005, **93**, (5), pp. 892–906
- 3 Taylor, C.W., Venkatasubramanian, M.V., and Chen, Y.: 'Wide-area stability and voltage control'. Proc. VII Symp. Specialists in Electric Operational and Expansion Planning, 2000, pp. 1–9
- 4 Taylor, C.W.: 'The future in on-line security assessment and wide-area stability control'. IEEE Power Engineering Society Winter Meeting, 2000, vol. 1, pp. 78–83
- 5 Hauer, J.F., Mittelstadt, W.A., and Adapa, R.: 'Chapter 11: power system dynamics and stability. Section 8: direct analysis of wide area dynamics' (CRC Electric Power Engineering Handbook, CRC Press, Cleveland, OH, 2000)
- 6 Kamwa, I., and Grondin, R.: 'PMU configuration for system dynamic performance measurement in large, multiarea power systems', *IEEE Trans. Power Syst.*, 2002, **17**, (2), pp. 385–394
- 7 Wilson, R.E., and Taylor, C.W.: 'Using dynamic simulations to design the wide-area stability and voltage control system (WACS)'. IEEE Power Syst. Conference and Exposition, 2004, vol. 1, pp. 100–107
- 8 Aboul-Ela, M.E., Sallam, A.A., McCalley, J.D., and Fouad, A.A.: 'Damping controller design for power system oscillations using global signals', *IEEE Trans. Power Syst.*, 1996, **11**, pp. 767–773
- 9 Zima, M., Larsson, M., Korba, P., Rehtanz, C., and Andersson, G.: 'Design aspects for wide-area monitoring and control Systems', *Proc. IEEE*, 2005, **93**, (5), pp. 980–996
- 10 Karlsson, D., Hemmingsson, M., and Lindahl, S.: 'Wide area system monitoring and control – terminology, phenomena, and solution implementation strategies', *IEEE Power Energy Mag.*, 2004, **2**, (5), pp. 68–76

- 11 Choudhuri, B., Majumder, R., and Pal, B.C.: 'Application of multiple-model adaptive control strategy for robust damping of interarea oscillations in power system', *IEEE Trans. Control Syst. Technol.*, 2004, **12**, (5), pp. 727–736
- 12 Okou, F., Dessaint, L.A., and Akhrif, O.: 'Power systems stability enhancement using a wide-area signals based hierarchical controller', *IEEE Trans. Power Syst.*, 2005, **20**, (3), pp. 1465–1477
- 13 Hongxia, W., Hui, N., and Heydt, G.T.: 'The impact of time delay on robust control design in power systems'. IEEE Power Engineering Society Winter Meeting, 2002, vol. 2, pp. 1511–1516
- 14 Snyder, A.F., Ivanescu, D., HadjSaid, N., Georges, D., and Margotin, T.: 'Delayed-input wide area stability control with synchronized phasor measurements and linear matrix inequalities'. IEEE Power Engineering Society Summer Meeting, 2000, vol. 2, pp. 1009–1014
- 15 Hongxia, W., Tsakalis, K.S., and Heydt, G.T.: 'Evaluation of time delay effects to wide-area power system stabilizer design', *IEEE Trans. Power Syst.*, 2004, **19**, (4), pp. 1935–1941
- 16 Hongxia, W., and Heydt, G.T.: 'Design of delayed-input wide area power system stabilizer using the gain scheduling method'. IEEE Power Engineering Society General Meeting, 2003, vol. 3, pp. 1704–1709
- 17 Chaudhuri, B., Majumder, R., and Pal, B.C.: 'Wide-area measurement-based stabilizing control of power system considering signal transmission delay', *IEEE Trans. Power Syst.*, 2004, **19**, (4), pp. 1971–1979
- 18 Majumder, R., Pal, B.C., Dufour, C., and Korba, P.: 'Design and real-time implementation of robust FACTS controller for damping inter-area oscillation', *IEEE Trans. Power Syst.*, 2006, **21**, (2), pp. 809–816
- 19 Amin, S.M., and Wollenberg, B.F.: 'Toward a smart grid', *IEEE Power Energy Mag.*, 2005, **3**, (5), pp. 34–41
- 20 Park, J.W., Harley, R.G., and Venayagamoorthy, G.K.: 'MLP/RBF neural networks based on-line global model identification of synchronous generator', *IEEE Trans., Ind. Electr.* 2005, **52**, (6), pp. 1685–1695
- 21 Venayagamoorthy, G.K., and Harley, R.G.: 'Two separate continually online-trained neurocontrollers for excitation and turbine control of a turbogenerator', *IEEE Trans. Ind. Appl.*, 2002, **38**, (3), pp. 887–893
- 22 Klein, M., Rogers, G.J., and Kundur, P.: 'A fundamental study of inter-area oscillations in power systems', *IEEE Trans. Power Syst.*, 1991, **6**, (3), pp. 914–921
- 23 Kundur, P.: 'Power system stability and control' (McGraw-Hill, New York, 1994)
- 24 Forsyth, P., Maguire, T., and Kuffel, R.: 'Real time digital simulation for control and protection system testing'. IEEE 35th Annual Power Electronics Specialists Conf., 2004, vol. 1, pp. 329–335
- 25 Serpen, G., Patwardhan, A., and Geib, J.: 'The simultaneous recurrent neural network addressing the scaling problem in static optimization', *Int. J. Neural Syst.*, 2001, **11**, (5), pp. 477–487
- 26 Werbos, P.J., and Pang, X.: 'Generalization maze navigation: SRN critic solve what feedforward or hebbian nets cannot'. Proc. World Congress on Neural Networks, 1996, pp. 88–93
- 27 Narendra, K.S., and Parthasarathy, K.: 'Identification and control of dynamical systems using neural networks', *IEEE Trans. Neural Netw.*, 1990, **1**, (1), pp. 4–27
- 28 Shamsollahi, P., and Malik, O.P.: 'An adaptive power system stabilizer using on-line trained neural networks', *IEEE Trans. Energy Convers.*, 1997, **12**, (4), pp. 382–387
- 29 Zhou, N., Pierre, J.W., and Hauer, J.F.: 'Initial results in power system identification from injected probing signals using a subspace method', *IEEE Trans. Power Syst.*, 2006, **21**, (3), pp. 1296–1302
- 30 Pierre, J.W., Trudnowski, D.J., and Donnelly, M.K.: 'Initial results in electromechanical mode identification from ambient data', *IEEE Trans. Power Syst.*, 1997, **12**, (3), pp. 1245–1251
- 31 OMNIBUS User's Manual, Innovative Integration, CA USA, 2001
- 32 Hauer, J.F.: 'Application of Prony analysis to the determination of modal content and equivalent models for measured power system response', *IEEE Trans. Power Syst.*, 1991, **6**, (3), pp. 1062–1068
- 33 Hong, J.H., and Park, J.K.: 'A time-domain approach to transmission network equivalents via Prony analysis for electromagnetic transients analysis', *IEEE Trans. Power Syst.*, 1995, **10**, (4), pp. 1789–1797

9 Appendix

Generators G1–G4:

- Rated MVA of the machine = 900.0 MVA.
- Rated RMS line-to-line voltage = 20 kV.
- Base angular frequency = 60.0 Hz.

Generator parameters

Generator	H	Ra, pu	Xa, pu	Xd, pu	Xd', pu	Xd'', pu	Xq, pu	Xq', pu	Xq'', pu	Td0', pu	Td0'', pu	Tq0', pu	Tq0'', pu
G1	6.5	0.0025	0.2	1.8	0.3	0.25	1.7	0.55	0.25	8.0	0.03	0.4	0.05
G2	6.5	0.0025	0.2	1.8	0.3	0.25	1.7	0.55	0.25	8.0	0.03	0.4	0.05
G3	6.175	0.0025	0.2	1.8	0.3	0.25	1.7	0.55	0.25	8.0	0.03	0.4	0.05
G4	6.175	0.0025	0.2	1.8	0.3	0.25	1.7	0.55	0.25	8.0	0.03	0.4	0.05

Exciter parameters for G1–G4

V _{rated} , KV	T _r , s	T _c , s	T _b , s	K _a	T _a , s	V _{rmax} , pu	V _{rmin} , pu	K _c	K _f	T _f , s
20.0	0.0	1.0	1.0	200.0	0.01	5.1	-4.0	0.0	0.0	1.0

PSS for G1–G4

K ₁	T _{wr} , s	T ₁ , s	T ₂ , s	T ₃ , s	T ₄ , s	V _{cu} , pu	V _{cl} , pu
20	10	0.05	0.02	3.0	5.4	1.2	0.2

Turbine/governor for G1–G4

R	T ₁ , s	T ₂ , s	T ₃ , s	Upper limit, pu	Lower limit, pu
0.05	0.36	2.16	8.0	1.07	0.0

Loadflow

Bus number	Rated voltage, kV	Bus type	Voltage, pu	Phase, degree
1	20.0	2	1.030	14.46
2	20.0	2	1.010	4.67
3	20.0	2	1.030	-23.32
4	20.0	2	1.010	-30.88
5	230.0	3	1.005	37.99
6	230.0	3	0.974	27.85
7	230.0	3	0.953	19.36
8	230.0	3	0.930	2.01
9	230.0	3	0.970	-14.91
10	230.0	3	0.984	-7.62
11	230.0	1	1.000	0.00

Load data

Bus number	Real power, MW	Reactive power, MVAR
7	967.09	0.00
7	0.00	99.91
9	0.00	250.00
9	1767.00	0.00

Generator operating data

Generator number	Real power, MW	Reactive power, MVAR
1	700.00	196.18
2	700.00	261.46
3	719.00	227.34
4	700.00	198.14

Branch or transmission line data

From bus	To bus	Resistance, pu	Reactance, pu	Succeptance, pu
10	11	0.0025	0.0250	0.0438
1	4	0.0000	0.0167	0.0000
3	11	0.0000	0.0167	0.0000
5	6	0.0025	0.0250	0.0438
1	5	0.0000	0.0167	0.0000
2	6	0.0000	0.0167	0.0000
6	7	0.0010	0.0100	0.0175
7	8	0.0110	0.1100	0.1925
7	8	0.0110	0.1100	0.1925
8	9	0.0110	0.1100	0.1925
8	9	0.0110	0.1100	0.1925
9	10	0.0010	0.0100	0.0175